Catalysis Today 213 (2013) 87–92

Contents lists available at SciVerse ScienceDirect

Catalysis Today

journal homepage: www.elsevier.com/locate/cattod

# Selective liquid-phase hydrogenation of furfural to furfuryl alcohol over Cu-based catalysts

M.M. Villaverde, N.M. Bertero, T.F. Garetto*, A.J. Marchi

*Catalysis Science and Engineering Research Group (GICIC), Instituto de Investigaciones en Catálisis y Petroquímica (INCAPE), FIQ-UNL, CONICET, Santiago del Estero 2654, 3000 Santa Fe, Argentina*

ARTICLE INFO

*Article history:*
Received 11 December 2012
Received in revised form 7 February 2013
Accepted 11 February 2013
Available online 17 April 2013

*Keywords:*
Furfural
Liquid-phase hydrogenation
Furfuryl alcohol
Cu-based catalysts

ABSTRACT

In this work, the liquid-phase furfural hydrogenation over different Cu-based catalysts was studied. The catalysts were prepared by incipient wetness impregnation ($Cu/SiO_2$-I), precipitation–deposition ($Cu/SiO_2$-PD) and co-precipitation (CuMgAl, CuZnAl and Cu-Cr) methods. CuMgAl, CuZnAl and $Cu/SiO_2$-PD showed higher Cu dispersion and $H_2$ chemisorption capacity than Cu-Cr and $Cu/SiO_2$-I. The selectivity to furfuryl alcohol, at 383 K and 10 bar, using 2-propanol as solvent, was 100% in all of the cases. The pattern for the hydrogenation rate per gram of Cu was: CuMgAl > $Cu/SiO_2$-PD > CuZnAl > Cu-Cr > $Cu/SiO_2$-I. Instead, the hydrogenation rate per Cu atom on the surface (TOF) followed the pattern: CuMgAl > Cu-Cr > $Cu/SiO_2$-PD ≅ CuZnAl > $Cu/SiO_2$-I. These are promising results for the future replacement of polluting Cu-Cr industrial catalysts by a Cr-free one. The highest activity of CuMgAl was attributed to an intimate and effective interaction between $Cu^0$ atoms and $Mg^{2+}$ cations in a spinel-like matrix. Additional catalytic tests, varying reactant initial concentration and temperature, were performed with CuMgAl catalyst. A negative reaction order (≅ −1) respect to furfural and a high apparent activation energy (≅ 127 KJ $mol^{-1}$) were estimated, indicating a very strong adsorption of furfural on metal copper surface.



## 1. Introduction

Furfuryl alcohol (FOL) is a very important intermediate in the chemical industry since it is widely used in the production of: (1) thermostatic resins with high chemical resistance to acids, bases and certain solvents; (2) liquid resins for galvanic bath; (3) synthetic fibers; (4) farm chemicals; (5) foundry binders; (6) adhesives for plywood and furniture; (7) other fine chemical products such as vitamin C and lysine [1–4]. FOL is mainly produced by furfural (FAL) hydrogenation either in gas or liquid phase. Gas-phase hydrogenation of FAL has mainly two disadvantages: higher amount of byproducts than those produced in the liquid-phase process and higher energy consumption due to the necessity of vaporizing FAL [5]. Instead, solvent and high $H_2$ pressures are required in liquid-phase FAL hydrogenation but generally high selectivity to FOL are reached [4,6].

It is well known that copper chromite (Cu-Cr) catalysts have been the most successful commercial catalysts for over five decades in FAL hydrogenation processes. Selectivities to FOL of 98% in liquid-phase and between 35 and 98% in gas-phase are achieved with this Cu-Cr catalyst in different industrial processes [4]. However, the main drawback of the Cu-Cr catalysts is their high toxicity that causes severe environmental pollution after catalyst final disposal [7]. Even more, though these catalysts are very selective to FOL, they showed a moderate activity for FAL hydrogenation [8]. Based on the previously said, it is a great challenge to design environmentally friendly, active and selective catalysts for the liquid-phase FAL hydrogenation to FOL.

Fig. 1 shows the most likely reaction pathways for FAL conversion over metal catalysts in the presence of $H_2$. Initially, three different reactions are possible: the selective hydrogenation of the carbonyl group of FAL to give FOL that is the desired reaction, the reduction of the C=C bonds to give tetrahydrofurfural (THFAL) and the decarbonylation of FAL to produce furan (FAN). These three primary products are then converted in several other compounds by different hydrogenation and hydrogenolysis reactions. For instance, THFAL and FOL can be converted by hydrogenation into tetrahydrofurfuryl alcohol (THFOL), which is also a product of industrial importance. Other possible reaction products could be 2-methylfuran (MFAN), 2-methyl-tetrahydrofuran (THMF), 2-pentanol (PNOL), 1,5-pentanodiol (PDOL), tetrahydrofuran (THF) and 1-butanol (BNOL), as it is shown in Fig. 1. However, among all the products in this complex reaction network, FOL is the most interesting and valuable one for the chemical industry, therefore important efforts are made in order to achieve high FOL selectivity.

The liquid-phase FAL hydrogenation has been studied using catalysts based on Ni [2,9,10], Co [6] and Pt [1,11] and in some cases a second metal or a promoter was added to improve the activity

* Corresponding author. Tel.: +54 342 4533858; fax: +54 342 4531068.
*E-mail addresses:* tgaretto@fiq.unl.edu.ar, tgaretto@gmail.com (T.F. Garetto).

0920-5861/$ – see front matter © 2013 Published by Elsevier B.V.
http://dx.doi.org/10.1016/j.cattod.2013.02.031

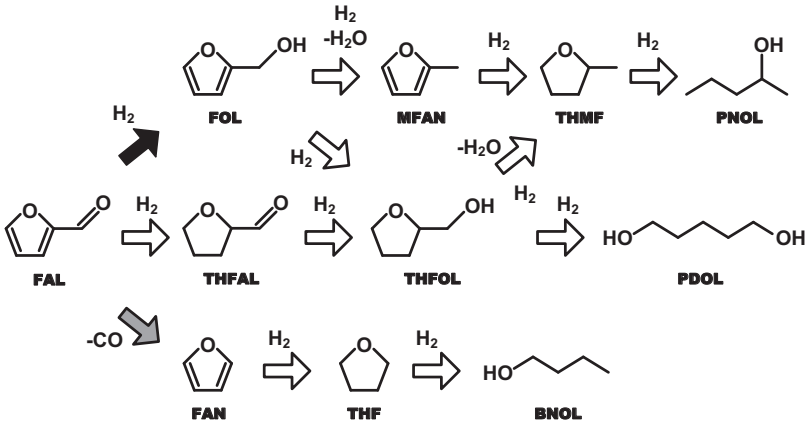


**Fig. 1.** Reaction pathways for the conversion of furfural (FAL) with $H_2$ in the presence of metallic catalysts.

and/or selectivity. Little information is available in the literature about the use of Cu-based catalysts containing no Cr for the FAL hydrogenation. Xu et al. studied the effect of the activation temperature on the performance of Cu-Ni-Mg-Al catalysts, obtaining FOL selectivities between 80 and 85% at 473 K and 10 bar using ethanol as solvent [3]. In previous studies, our research group has shown that Cu-based catalysts are efficient for the liquid-phase hydrogenation of different unsaturated carbonyl compounds to the corresponding unsaturated alcohol [12–14]. Therefore, it seems reasonable to study the liquid-phase hydrogenation of FAL over Cu-based catalysts without Cr to compare their performance with that one of a Cu-Cr sample.

In this paper, we studied the liquid-phase FAL hydrogenation over different Cu-based catalysts free of Cr and the results were compared with those obtained with a Cu-Cr catalyst. Experimental data were obtained by varying FAL concentration and reaction temperature. The goal of this work is to determine the feasibility of replacing polluting Cu-Cr catalysts by eco-compatible catalytic systems for the selective liquid-phase FAL hydrogenation.

## 2. Experimental

### 2.1. Catalyst preparation

A $Cu/SiO_2$ catalyst ($Cu/SiO_2$-I) was prepared by the incipient wetness impregnation method. Copper was deposited on commercial silica (Sigma–Aldrich grade 62, 99.7%) by adding dropwise a 0.6 M aqueous solution of $Cu(NO_3)_2{\cdot}3H_2O$ (Merck, 98%). The solid was dried in an oven at 373 K for 12 h and then decomposed in $N_2$ flow at 673 K for 5 h.

Another $Cu/SiO_2$ catalyst ($Cu/SiO_2$-PD) was prepared by the precipitation–deposition method, adding simultaneously an aqueous solution of $Cu(NO_3)_2{\cdot}3H_2O$ and an aqueous solution of $K_2CO_3$ at pH $7.2 \pm 0.2$ in an aqueous $SiO_2$ suspension at 333 K. After aging for 1 h at 333 K, the solid was separated by filtration, washed with deionized water at 333 K and dried at 353 K overnight. The hydrated precursor was then decomposed in $N_2$ flow at 673 K for 5 h to obtain the corresponding oxide precursor.

CuZnAl, CuMgAl and Cu-Cr catalysts were prepared by the co-precipitation method. An acidic solution containing the metal nitrates and an aqueous $K_2CO_3$ solution were simultaneously added dropwise to 400 mL of distilled water at 333 K, while keeping the pH at $7.2 \pm 0.2$ for CuZnAl and Cu-Cr or $10 \pm 0.2$ for CuMgAl, according to the procedures described elsewhere [15–17]. The resulting precipitates were aged for 1 h at 333 K and then filtered, washed with deionized water at 333 K and dried at 353 K overnight. The hydrated precursors were decomposed in $N_2$ flow at 773 K for 5 h to obtain the corresponding mixed oxides. The atomic ratios in CuZnAl and CuMgAl were (Cu + M)/Al = 1 and M/Al = 0.75, where M = Mg, Zn. In the case of Cu-Cr sample, the Cu/Cr ratio was equal to 20.

### 2.2. Catalyst characterization

The identification of polycrystalline species formed after decomposition in $N_2$ flow was carried out by X-ray diffraction (XRD) using a Shimadzu XD-1 diffractometer and Ni-filtered Cu-K$\alpha$ radiation with a scan speed of $2^\circ\,min^{-1}$. The crystallite sizes were estimated by applying Debye-Scherrer equation. Specific surface areas (Sg) were measured by $N_2$ physisorption at 77 K in a Quantochrome Autosorb I sorptometer. Elemental composition of the samples was determined by atomic absorption spectroscopy (AAS).

The relative reducibility of the calcined metal samples was determined by temperature-programmed reduction (TPR) using a Micromeritics AutoChem II 2920 V 2.00 equipment with a TCD detector. TPR profiles were obtained with a $H_2$(5%)/Ar gaseous mixture at 60 mL (STP) $min^{-1}$ through a fixed bed containing 100 mg of sample, while heating from 298 to 973 K at 10 K/min.

The metal dispersion of the Cu catalysts was measured by titration with $N_2O$ at 363 K using a stoichiometry of $(Cu^0)_s/N_2O = 2$, where $(Cu^0)_s$ is a $Cu^0$ atom on surface [18,19]. Pre-reduced samples were exposed to pulses of $N_2O$(10%)/Ar. The number of chemisorbed oxygen atoms was calculated from the consumption of $N_2O$ measured by mass spectrometry (MS) in a Baltzers Omnistar unit.

Hydrogen chemisorption was measured via volumetric adsorption experiments at room temperature in a conventional vacuum apparatus using a method described elsewhere [14].

### 2.3. Catalytic tests

The liquid-phase hydrogenation of FAL (Aldrich, 99%) was carried out in a 100 mL autoclave (Parr 4565), equipped with mechanical stirrer, in the range of 363–383 K and using 2-propanol (Merck, 99%) as solvent. The autoclave was loaded with 60 mL of solvent and about 0.1 g of catalyst. Prior to catalytic tests, samples were activated ex situ in $H_2$ flow (30 mL $min^{-1}$) at 623 K for 1.5 h and then transferred to the reactor, avoiding contact with air, under inert atmosphere ($N_2$). The reaction system was stirred and heated up to reaction temperature at 2 K/min. Then, 0.25–1.00 mL of FAL was injected into the reactor and the total pressure was rapidly increased up to 10 bar with $H_2$. The batch reactor was assumed to be perfectly mixed. A stirring speed higher than 600 rpm and catalyst particles smaller than 100 $\mu$m in size were used to ensure the

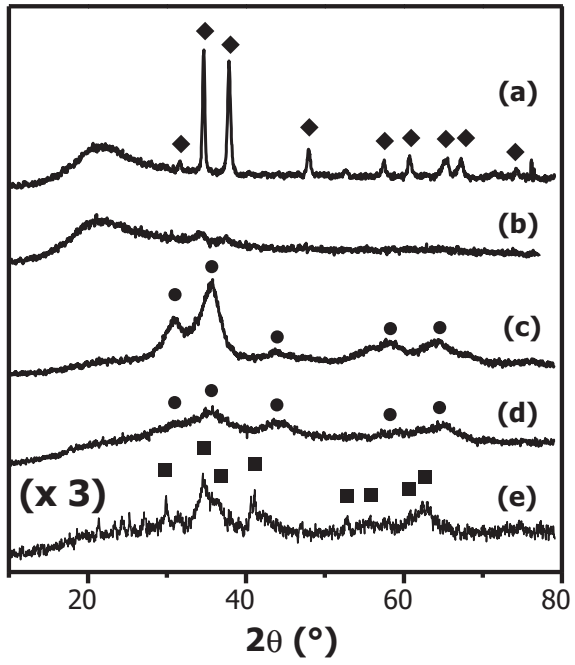


**Fig. 2.** Characterization of samples. X-ray diffraction patterns [scan speed: 2°/min]: (a) $Cu/SiO_2$-I; (b) $Cu/SiO_2$-PD; (c) CuZnAl; (d) CuMgAl; (e) Cu-Cr. Phases: (♦) CuO (tenorite-like); (●) spinel-like; (■) $CuCr_2O_4$ (spinel-like).

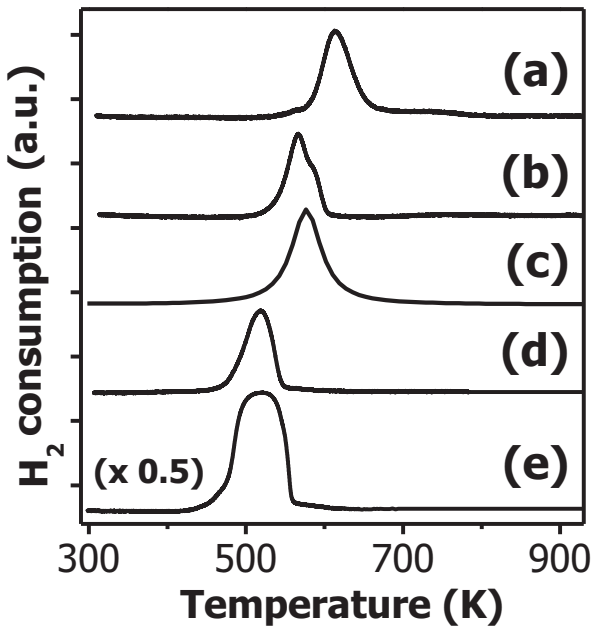


**Fig. 3.** Characterization of samples. TPR profiles [heating rate: 10 K/min]: (a) $Cu/SiO_2$-I; (b) $Cu/SiO_2$-PD; (c) CuZnAl; (d) CuMgAl; (e) Cu-Cr.

kinetic control of the reaction; i.e., diffusional limitations were negligible [13]. The absence of gas/liquid, liquid/solid and intraparticle mass transfer limitations was verified using the quantitative criteria described by Ramachandran and Chaudhari [20]. This criterion has been widely employed for liquid-phase hydrogenation reactions with successful results [21,22].

Concentrations of FAL and products were followed during the reaction by ex situ gas chromatography using an Agilent 6850 chromatograph equipped with flame ionization detector and a 30 m HP-Innowax capillary column with a 0.25 mm coating. Liquid samples were withdrawn from the reactor and collected every 15–30 min by using a loop under pressure in order to avoid flushing.

Reactant conversion ($X_{FAL}$, mol of FAL reacted/mol of FAL fed) was calculated as $X_{FAL} = (C^0_{FAL} - C_{FAL})/C^0_{FAL}$, where $C^0_{FAL}$ is the initial FAL concentration and $C_{FAL}$ is the FAL concentration at time $t$. Selectivities toward product $i$ ($S_i$, mol of product $i$/mol of converted reactant) were calculated as $S_i = C_i/\sum C_j$, where $\sum C_j$ is the total concentration of products. The $C_j$ values were calculated using n-dodecane (Sigma–Aldrich, >99%) as internal standard.

## 3. Results and discussion

### 3.1. Catalyst characterization

The results obtained from the characterization of samples used in this work are summarized in Table 1. The Cu loading for the catalysts without Cr, determined by AAS, was between 11 and 18 wt%, while for the Cu-Cr sample was 43.7 wt%. This is a Cu loading three to four times higher than for the Cr-free samples and similar to the Cu loading of commercial Cu-Cr catalysts. Thus, metal loading followed the trend: Cu-Cr > CuMgAl > CuZnAl ≅ $Cu/SiO_2$-I ≅ $Cu/SiO_2$-PD.

The X-ray diffractograms of the precursors after decomposition in $N_2$ are shown in Fig. 2. $Cu/SiO_2$-I sample contains a single polycrystalline phase with a tenorite-like structure (CuO, JCPDS 5-0661), obtained by decomposition of $Cu(NO_3)_2$ (JCPDS 14-415), with a mean crystallite size of about 30 nm. No X-ray diffraction signals were observed in the case of $Cu/SiO_2$-PD oxide precursor, suggesting that the CuO phase is quasi-amorphous (q.a.) and/or formed by small crystalline domains that are not detectable by XRD (Table 1, Fig. 2). In the case of the samples prepared by co-precipitation, the only polycrystalline phase detected by XRD after decomposition in $N_2$ was a spinel-like phase ($ZnAl_2O_4$, JCPDS 5-0669 and $MgAl_2O_4$, JCPDS 21-1152), which was obtained by pseudomorphic decomposition of a hydrotalcite-like phase (JCPDS 14-191) formed during co-precipitation [23]. For both cases, the spinel-like phase showed a low crystallinity degree and small mean crystallite size of about 5 nm. No segregation of CuO, ZnO or MgO crystalline phases were detected in the CuZnAl and CuMgAl mixed oxides after decomposition, thereby indicating that the cations are highly dispersed in the spinel-like matrix. Finally, the only polycrystalline phase detected for the Cu-Cr sample was $CuCr_2O_4$, which also has a spinel-like structure (JCPDS 5-0657).

The specific surface areas (Sg) of the oxide precursors without Cr were between 170 and 291 $m^2\,g^{-1}$ (Table 1). In particular, the silica-supported samples $Cu/SiO_2$-I and $Cu/SiO_2$-PD showed specific surface areas slightly lower than the one corresponding to the $SiO_2$ support (230 $m^2\,g^{-1}$). The Cr-free mixed oxides with spinel-like structure showed specific surface areas of 171 $m^2\,g^{-1}$ for CuZnAl and 291 $m^2\,g^{-1}$ for CuMgAl. In contrast, the specific surface area of the Cu-Cr oxide precursor was about only a quarter of those values determined for the silica-supported samples. In summary, the specific surface area trend was: CuMgAl > $Cu/SiO_2$-PD ≅ $Cu/SiO_2$-I > CuZnAl ≫ Cu-Cr.

The results corresponding to the reducibility of the samples after decomposition in $N_2$ are shown in Fig. 3 and Table 1. The TPR profile for the $Cu/SiO_2$-I oxide precursor exhibited only a broad peak between 573 and 663 K, with the maximum at 613 K, arising from the reduction of the tenorite-like phase [Fig. 3, profile (a)]. This broad peak is indicating the reduction of CuO particles with a wide size distribution, as it has been previously suggested [15]. The TPR experiment with $Cu/SiO_2$-PD sample [Fig. 3, profile (b)] showed a reduction profile shifted to lower temperatures, between 523 and 603 K, with the maximum at 569 K and a shoulder at 583 K. This TPR profile is suggesting a broad size distribution of CuO particles rather different to that of $Cu/SiO_2$-I [24]. It is also possible that $Cu^{2+}$ ions on $Cu/SiO_2$-PD are interacting in dissimilar grade with

**Table 1**
Physicochemical characterization of the Cu-based catalysts.

| Sample | Cu load[a] (wt%) | Hydrated precursor[b] | Metal oxide[b] | $S_g$ ($m^2\ g^{-1}$) | TPR $T_{MAX}$[c] (K) | $D_M$[d] (%) | $V_{H2}$[e] ($l_{STP}/mol_s$) |
|---|---|---|---|---|---|---|---|
| $Cu/SiO_2$-I | 11.4 | $Cu(NO_3)_2$ | CuO | 221 | 615 | 2 | 0.45 |
| $Cu/SiO_2$-PD | 11.3 | q.a. | q.a. | 225 | 569 | 21 | 0.38 |
| CuZnAl | 12.9 | Hydrotalcite | Spinel | 171 | 534 | 23 | 0.53 |
| CuMgAl | 17.9 | Hydrotalcite | Spinel | 291 | 519 | 11 | 0.92 |
| Cu-Cr | 43.7 | q.a. | $CuCr_2O_4$ | 53 | 520 | 3 | 0.45 |

[a] Cu loading determined by atomic absorption spectroscopy (AAS) and verified by temperature programmed reduction (TPR).
[b] Polycrystalline phases identified by XRD.
[c] Reduction temperature at the maximum $H_2$ consumption in TPR experiments.
[d] Metal dispersion by titration with $N_2O$ at 363 K.
[e] Volume of irreversibly chemisorbed hydrogen at room temperature referred to surface metal copper.

silica support surface. As a consequence, $Cu^{2+}$ ions with varying reducibility will be present on the support surface. In any case, an asymmetric TPR profile, as the one shown in Fig. 3(b), will be obtained. Assuming a core-shell model for the reduction, it is likely that the CuO particles of $Cu/SiO_2$-PD are much smaller than those of $Cu/SiO_2$-I, in agreement with XRD results. This is explaining the lower reduction temperature in the case of $Cu/SiO_2$-PD [Fig. 3, profiles (b) and (a)]. The TPR profile of CuZnAl mixed oxide showed a single and broad reduction peak between 483 and 623 K with the maximum at 575 K [Fig. 3, profile (c)]. This reduction peak is suggesting an important Cu-support interaction and a size distribution similar to the case of $Cu/SiO_2$-PD sample. CuMgAl, the other Cr-free mixed oxide prepared by the co-precipitation method, showed also a single reduction peak but at lower temperatures than CuZnAl, more specifically between 463 and 553 K, with the maximum at 519 K [Fig. 3, profile (d)]. This is indicating a $Cu^{2+}$-support interaction and/or a size distribution of CuO particles some different to those ones in CuZnAl and $Cu/SiO_2$-PD. No evidence of $CuAl_2O_4$ reduction was detected in CuZnAl and CuMgAl samples, which is consistent with XRD characterization results. Finally, the Cu-Cr sample exhibited a large and very broad reduction peak between 453 and 563 K, showing the maximum at 520 K [Fig. 3, profile (e)]. In summary, the pattern for the reducibility of the oxide samples was: CuMgAl ≅ Cu-Cr > CuZnAl ≅ $Cu/SiO_2$-PD > $Cu/SiO_2$-I. Assuming a $CuO/H_2 = 1$ stoichiometric, Cu loads determined by AAS were verified with the total $H_2$ consumption estimated from the TPR profiles. In addition, after reduction at 623 K in a $H_2$(100%) flow for 1.5 h, it was verified that there was no further $H_2$ consumption. This result is indicating complete reduction of $Cu^{2+}$ ions to $Cu^0$ in all of the samples.

The capacity for irreversible $H_2$ chemisorption, on the basis of the exposed metal surface, followed the pattern: CuMgAl > CuZnAl > Cu-Cr ≅ $Cu/SiO_2$-I > $Cu/SiO_2$-PD. It is worth noticing that the values determined for Cu-Cr, CuZnAl, $Cu/SiO_2$-PD and $Cu/SiO_2$-I were about half of that one for CuMgAl (Table 1). This is indicating that the CuMgAl sample, with the highest $Cu^{2+}$ reducibility of the Cr-free series, has also the highest capacity for the dissociative $H_2$ chemisorption.

Regarding the copper dispersion, the results of the titration with $N_2O$ at 363 K are presented in Table 1. Samples $Cu/SiO_2$-PD and CuZnAl showed dispersion values (21–23%) twice higher than that for CuMgAl sample (11%) and one order of magnitude higher than those for $Cu/SiO_2$-I and Cu-Cr (2–3%). Therefore, the metallic dispersion pattern was: CuZnAl ≅ $Cu/SiO_2$-PD > CuMgAl > Cu-Cr ≅ $Cu/SiO_2$-I. In the case of $Cu/SiO_2$-I and $Cu/SiO_2$-PD it was possible to estimate the average particle size assuming cubic metal particles and using a surface density of Cu atoms of $1.08 \times 10^{15}$ at $cm^{-2}$. The estimated values for the Cu metal particle size were 32 nm for $Cu/SiO_2$-I and 3.3 nm for $Cu/SiO_2$-PD. This is in agreement with XRD and TPR results (Figs. 2 and 3) and it is indicating that small metal copper particles are formed by reduction of the highly dispersed CuO phase on $Cu/SiO_2$-PD. In contrast, large metal particles are obtained from the reduction of a poorly dispersed CuO phase in $Cu/SiO_2$-I.

### 3.2. Catalytic tests

#### 3.2.1. Screening of Cu-based catalysts

FAL conversion evolutions, in function of the parameters ($W_{Cu}.t/n^0_{FAL}$) and ($Cu_{exp}.t/m^0_{FAL}$), are shown in Fig. 4. The initial FAL conversion rates ($r^0_{FAL}$, $mol\ g^{-1}{}_{Cu}\ min^{-1}$) and turnover frequencies (TOF, $min^{-1}$) were estimated by applying polynomial differentiation at zero time to these curves in Fig. 4(a) and (b), respectively. These $r^0_{FAL}$ and TOF values are presented in Table 2. The pattern for the initial hydrogenation rate ($r^0_{FAL}$) was: CuMgAl > $Cu/SiO_2$-PD > CuZnAl > Cu-Cr » $Cu/SiO_2$-I (Fig. 4(a) and Table 2); i.e. three of the Cr-free catalysts were initially more active than Cu-Cr sample. However, taking into account the differences in Cu dispersion and loading among the samples, it becomes necessary to estimate TOF values in order to compare the intrinsic activity of the Cu metal sites. Considering the TOF values, the activity pattern was: CuMgAl > Cu-Cr > $Cu/SiO_2$-PD ≅ CuZnAl > $Cu/SiO_2$-I (Fig. 4(b) and Table 2). It is worth noticing that TOF for CuMgAl catalyst was twice of that for Cu-Cr and about one order of magnitude higher than those for CuZnAl and $Cu/SiO_2$ catalysts. This pattern is in agreement with the one determined from FAL conversions after 4 h of reaction, also shown in Table 2. In addition, when the initial FAL concentration was increased twice, the FAL conversion at 4 h of reaction clearly diminished for all the catalysts. This is suggesting that the FAL concentration has a negative effect on the reaction kinetic; i.e. the reaction order respect to FAL could be negative, reflecting a strong interaction between reactant and Cu metal surface. It is worth to notice that for CuZnAl and CuMgAl the conversion at 4 h diminished only 30–35% with the increase of the initial FAL concentration. Instead, the conversion decay was 50% for Cu-Cr, 70% with $Cu/SiO_2$-PD and 80% for $Cu/SiO_2$-I considering the same increase in the initial FAL concentration (Table 2).

The above results indicate that CuMgAl, with the highest $H_2$ chemisorption capacity, was the most active catalyst. However,

**Table 2**
Catalytic performance of Cu-based catalysts in liquid-phase FAL hydrogenation [$T$ = 383 K, $p$ = 10 bar, $W_{CAT}$ = 0.10 g, $V_{SOLV}$ = 60 mL (2-propanol)].

| Catalyst | $r^0_{FAL}$[a] ($mol\ g^{-1}{}_{Cu}\ min^{-1}$) | TOF[b] ($min^{-1}$) | $X_{FAL}$[c] (%) | $X_{FAL}$[d] (%) |
|---|---|---|---|---|
| $Cu/SiO_2$-I | $3.15 \times 10^{-5}$ | 0.10 | 4.8 | 0.8 |
| $Cu/SiO_2$-PD | $1.82 \times 10^{-3}$ | 0.55 | 66.3 | 21.4 |
| CuZnAl | $1.37 \times 10^{-3}$ | 0.38 | 48.1 | 33.3 |
| CuMgAl | $5.09 \times 10^{-3}$ | 2.94 | 100 | 65.7 |
| Cu-Cr | $6.28 \times 10^{-4}$ | 1.33 | 93.2 | 48.3 |

[a] Initial conversion rate of furfural referred to copper load.
[b] Turnover frequency.
[c] Conversion of furfural after 4 h of reaction for $C^0_{FAL} = 9.9 \times 10^{-2}$ M.
[d] Conversion of furfural after 4 h of reaction for $C^0_{FAL} = 2.0 \times 10^{-1}$ M.

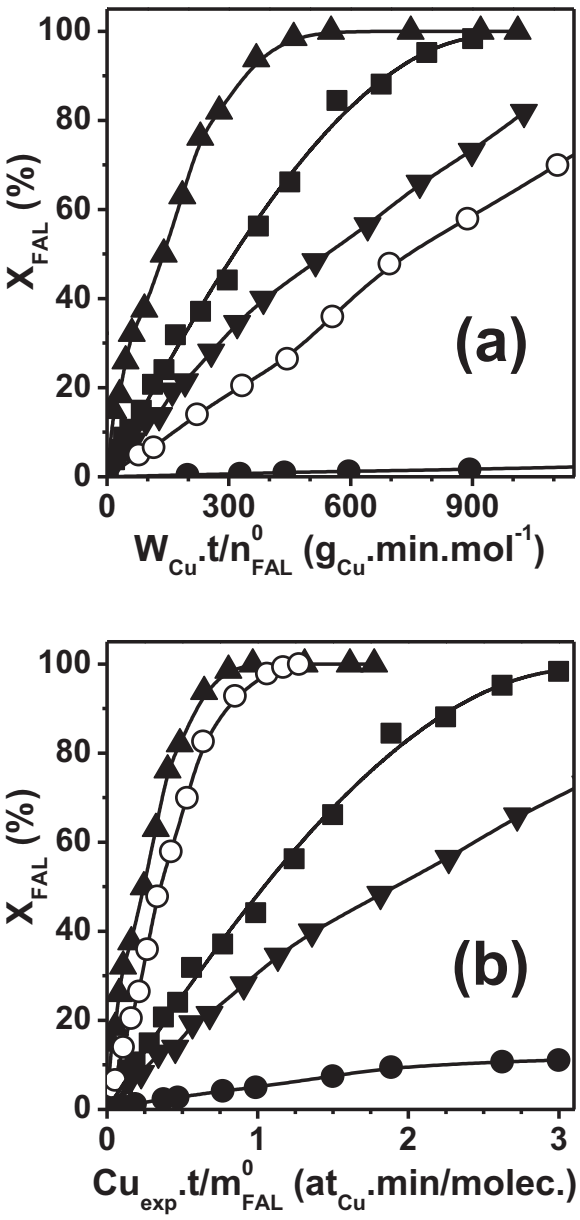


**Fig. 4.** Liquid-phase furfural (FAL) hydrogenation over Cu catalysts. (a) FAL conversion as a function of $W_{Cu}$ $t/n^0_{FAL}$; (b) FAL conversion as a function of $Cu_{exp}.t/m^0_{FAL}$. (▲) CuMgAl; (◯) Cu-Cr; (■) $Cu/SiO_2$-PD; (▼) CuZnAl; (●) $Cu/SiO_2$-I [$T$ = 383 K, $p$ = 10 bar, $W_{CAT}$ = 0.10 g, $C^0_{FAL} = 9.9 \times 10^{-2}$ M, $V_{SOLV}$ = 60 mL (2-propanol)].

considering all the samples, there is not a linear relationship between the activity pattern and $H_2$ chemisorption capacity or metal dispersion (Tables 1 and 2). This could indicate that the initial activity for FAL hydrogenation is also depending on the particular interaction between FAL and Cu metal surface in each case. In this sense, it is likely that metal active sites can chemisorb FAL strongly, partially poisoning the catalytic surface. This is in agreement with the decrease of the FAL hydrogenation rate as the initial FAL concentration increases (Table 2). This decrease in activity follows the pattern: $Cu/SiO_2$-I > $Cu/SiO_2$-PD > Cu-Cr > CuMgAl ≅ CuZnAl (Table 2). Thus, activity of samples with a spinel-like structure is less influenced by the increase in FAL concentration than activity of samples in which Cu is supported on $SiO_2$.

In summary, the initial activity and the decay in activity with the increase of reactant concentration are strongly influenced by different factors as $H_2$ chemisorption capacity, metal copper dispersion, catalyst structure and metal-support interaction. A higher dispersion of metal copper phase was attained on $Cu/SiO_2$-PD than on $Cu/SiO_2$-I. Thus, linear adsorption of FAL and dissociative chemisorption of hydrogen are more favored on $Cu/SiO_2$-PD than on $Cu/SiO_2$-I. This can explain the higher hydrogenation activity and the lower activity decay of $Cu/SiO_2$-PD respect to $Cu/SiO_2$-I. In the case of CuZnAl and CuMgAl, the high interaction of small metal copper particles with a spinel-like phase can modify the metal electronic density and/or the crystallographic planes exposed on the metal particle surface. In any case, the effect of this interaction on the copper catalytic activity is more important for CuMgAl than for CuZnAl. In other words, the nature of cations in the spinel plays a very important role. In this sense, $Mg^{2+}$ ions seem to favor the formation of a catalytic surface more active for FAL chemisorption and the subsequent hydrogenation than $Zn^{2+}$ ions. On the other hand, additional centers for on-top FAL adsorption can be available on the spinel-like surface [15]. Thus, FAL can be chemisorbed and activated on both small metal copper clusters and cations present on the surface of a non-stoichiometric spinel-like matrix. This increases the probability for FAL hydrogenation and decreases the deactivation effect by strong FAL adsorption on metal copper sites.

**Table 3**
Influence of the experimental conditions on the catalytic performance of CuMgAl in furfural (FAL) hydrogenation [$p$ = 10 bar, $W_{CAT}$ = 0.10 g, $V_{SOLV}$ = 60 mL (2-propanol)].

| Experimental condition | | $r^{*0}_{FAL}$[a] (mol g$^{-1}$ min$^{-1}$) | $X_{FAL}$[b] (%) |
|---|---|---|---|
| $C^0_{FAL}$ (M) ($T$ = 383 K) | $9.9 \times 10^{-2}$ | $9.67 \times 10^{-4}$ | 63.2 |
| | $1.2 \times 10^{-1}$ | $8.10 \times 10^{-4}$ | 44.5 |
| | $1.5 \times 10^{-1}$ | $6.53 \times 10^{-4}$ | 25.1 |
| T (K) | 363 | $1.08 \times 10^{-4}$ | 9.4 |
| ($C^0_{FAL} = 9.9 \times 10^{-2}$ M) | 373 | $3.12 \times 10^{-4}$ | 17.4 |
| | 383 | $9.67 \times 10^{-4}$ | 63.2 |

[a] Initial furfural conversion rate referred to total catalyst weight.
[b] Furfural conversion after 1 h of reaction.

Regarding the product distribution, it is worth noticing that selectivity to FOL was 100% in all of the cases during the complete catalytic runs. This is quite remarkable, taking into account the wide variety of products that can be formed from the interaction of FAL, $H_2$ and a metal catalyst, as it was shown in Fig. 1. In this sense, compared with other metal-based catalysts, Cu catalysts achieved total FOL selectivity without adding any other metal or promoter.

In summary, all the Cu-based catalysts used in this work were totally selective to FOL. However, CuMgAl was the most active catalyst of this series, which was attributed to a strong and intimate interaction between small metal copper particles and $Mg^{2+}$ ions on the surface of a non-stoichiometric spinel-like matrix. Then, this catalyst was selected to study the influence of the operative conditions on the catalytic activity.

### 3.2.2. Influence of reaction conditions

The effect of initial FAL concentration and temperature on the activity of CuMgAl catalyst, at constant $H_2$ pressure, was studied in this part. For this study, the initial FAL hydrogenation rate ($r^{*0}_{FAL}$) was expressed by g of catalyst (mol g$^{-1}$ min$^{-1}$) and a pseudo-homogeneous kinetic model based on a power-law rate equation was proposed (Eq. (1)).

$$r^{*0}_{FAL} = k \cdot (p_{H2})^{\alpha} \cdot (C^0_{FAL})^{\beta} = k' \cdot (C^0_{FAL})^{\beta} \quad (1)$$

The effect of FAL initial concentration on catalytic activity was studied at 383 K and 10 bar. The initial concentration of FAL ($C^0_{FAL}$) was varied between $9.9 \times 10^{-2}$ and $1.5 \times 10^{-1}$ M. The results, presented in Fig. 5(a) and Table 3, show that the initial catalytic activity decreases by increasing the initial FAL concentration, in agreement with the results previously obtained during the catalyst screening. The reaction order with respect to FAL was determined

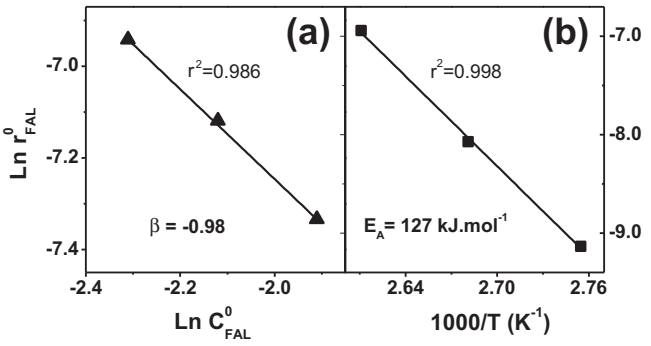


**Fig. 5.** Influence of (a) FAL initial concentration [$T$ = 383 K, $p$ = 10 bar] and (b) reaction temperature [$p$ = 10 bar, $C^0_{FAL} = 9.9 \times 10^{-2}$ M] on the catalytic activity in liquid-phase FAL hydrogenation over CuMgAl [$W_{CAT}$ = 0.10 g, $V_{SOLV}$ = 60 mL (2-propanol)].

by calculating β from these data applying both linear and non-linear regression with Eq. (1). The value estimated for β was equal to −0.98; i.e. a negative and almost unitary reaction order. A similar study performed with Cu-Cr catalyst at the same conditions gave a value for β approximately equal to −0.8 (not shown in this work). These results confirm that FAL interacts strongly with the Cu metal surface under the conditions used in this work.

The influence of temperature on catalytic activity was investigated between 363 and 383 K, at $p$ = 10 bar and $C^0_{FAL} = 9.9 \times 10^{-2}$ M. Taking into account that FAL is strongly adsorbed on metal copper surface and that the rate constant increases and the FAL adsorption constant diminishes with temperature, it is expected that the temperature will have an important impact on the FAL hydrogenation rate. The magnitude of the increase of the initial FAL hydrogenation rate with temperature is shown in Fig. 5(b) and Table 3. An estimate of 127 kJ mol$^{-1}$ for the apparent activation energy ($E_A$) was determined by numerical regression assuming valid Arrhenius law. To our knowledge, there are not many reported values for the activation energy of the liquid-phase FAL hydrogenation. Vaidya and Mahajani, using a Pt/C catalyst and 2-propanol as solvent, reported a value equal to 28 kJ mol$^{-1}$, which is a surprisingly low value considering that the absence of diffusional resistances was verified [1]. Rojas et al. reported an $E_A$ = 37.7 kJ mol$^{-1}$ for FAL hydrogenation over Ir/$Nb_2O_5$ catalyst [25]. In this sense, the values obtained for $E_A$ over noble metal-based catalysts, which are very active for this reaction, are much lower than the $E_A$ observed with CuMgAl catalyst. It is likely that the high $E_A$ estimated in this work is due to very strong adsorption of FAL on metal copper surface, as it was mentioned above. Then, temperature simultaneously increases the rate constant and diminishes the strong FAL adsorption over $Cu^0$ metal sites.

Regarding the catalyst selectivity, in all the catalytic runs the FOL selectivity was always equal to 100%, which shows that the CuMgAl catalyst is totally selective for hydrogenating FAL to FOL in this range of experimental conditions.

In summary, the negative order respect to FAL and the high apparent activation energy obtained in the liquid phase hydrogenation of FAL over CuMgAl are confirming the very strong interaction between reactant molecules and metal copper surface.

## 4. Conclusions

We have shown that Cu-based catalysts free of Cr are active for the liquid-phase hydrogenation of furfural with 100% selectivity to furfuryl alcohol. In particular, a CuMgAl catalyst, prepared by the coprecipitation method, was more active for this reaction than a copper chromite traditional catalyst. This could be a very important progress for the industrial production of furfuryl alcohol since, for many decades, the copper chromite catalysts were the most active and selective for this reaction.

A solid catalyst formed by small copper particles is more active and stable in the liquid-phase hydrogenation of furfural than when it is mainly constituted by large metal copper particles. This is clearly concluded from the comparison of Cu/$SiO_2$ catalysts prepared by precipitation–deposition and impregnation methods. However, metal-support interaction can also play a very important role in modifying the activity of metal copper. Thus, the catalytic performance is greatly improved if small copper particles are in intimate interaction with a Mg-Al spinel-like matrix.

It was also determined that it is desirable to work at high temperature in order to reach high furfural conversion rates and to reduce deactivation due to strong furfural adsorption. Selectivity to furfuryl alcohol is not influenced neither by initial furfural concentration nor temperature in this range of operative conditions, being always equal to 100%.

## Acknowledgements

We thank Universidad Nacional del Litoral (UNL), Consejo Nacional de Investigaciones Científicas y Técnicas (CONICET) and Agencia Nacional de Promoción Científica y Tecnológica (ANPCyT), Argentina, for the financial support to this work.

## References

[1] P.D. Vaidya, V.V. Mahajani, Industrial and Engineering Chemistry Research 42 (2003) 3881–3885.
[2] H. Li, S. Zhang, H. Luo, Materials Letters 58 (2004) 2741–2746.
[3] C. Xu, L. Zheng, D. Deng, J. Liu, S. Liu, Catalysis Communications 12 (2011) 996–999.
[4] A. Corma, S. Iborra, A. Velty, Chemical Reviews 107 (2007) 2411–2502.
[5] H.Y. Zheng, Y.L. Zhu, B.T. Teng, Z.Q. Bai, C.H. Zhang, H.W. Xiang, Y.W. Li, Journal of Molecular Catalysis A: Chemical 246 (2006) 18–23.
[6] X. Chen, H. Li, H. Luo, M. Qiao, Applied Catalysis A-General 233 (2002) 13–20.
[7] B.M. Nagaraja, A.H. Padmasri, B. David Raju, K.S. Rama Rao, Journal of Molecular Catalysis A: Chemical 265 (2007) 90–97.
[8] J. Wu, Y. Shen, C. Liu, H. Wang, C. Geng, Z. Zhang, Catalysis Communications 6 (2005) 633–637.
[9] B. Liu, L. Lu, B. Wang, T. Cai, K. Iwatani, Applied Catalysis A-General 171 (1998) 117–122.
[10] H. Li, H. Luo, L. Zhuang, W. Dai, M. Qiao, Journal of Molecular Catalysis A: Chemical 203 (2003) 267–275.
[11] A.B. Merlo, V. Vetere, J.F. Ruggera, M.L. Casella, Catalysis Communications 10 (2009) 1665–1669.
[12] N.M. Bertero, C.R. Apesteguía, A.J. Marchi, Catalysis Today 172 (2011) 171–176.
[13] N.M. Bertero, C.R. Apesteguía, A.J. Marchi, Applied Catalysis A-General 349 (2008) 100–109.
[14] A.J. Marchi, J.F. Paris, N.M. Bertero, C.R. Apesteguía, Industrial and Engineering Chemistry Research 46 (2007) 7657–7666.
[15] A.J. Marchi, D.A. Gordo, A.F. Trasarti, C.R. Apesteguía, Applied Catalysis A-General 249 (2003) 53–67.
[16] J.I. Di Cosimo, V.K. Diez, M. Xu, E. Iglesia, C.R. Apesteguía, Journal of Catalysis 178 (1998) 499–510.
[17] S. Abello, S. Dhir, G. Colet, J. Pérez-Ramírez, Applied Catalysis A-General 325 (2007) 121–129.
[18] A. Dandekar, M.A. Vannice, Journal of Catalysis 178 (1998) 621–639.
[19] M.H. Kim, J.R. Ebner, R.M. Friedman, M.A. Vannice, Journal of Catalysis 208 (2002) 381–392.
[20] P.A. Ramachandran, R.V. Chaudhari, Three Phase Catalytic Reactors, Gordon and Breach, New York, 1983.
[21] M.V. Rajashekharam, I. Bergault, P. Fouilloux, D. Schweich, H. Delmas, R.V. Chaudhari, Catalysis Today 48 (1999) 83–92.
[22] R.V. Malyala, C.V. Rode, M. Arai, S.G. Hegde, R.V. Chaudhari, Applied Catalysis A-General 193 (2000) 71–86.
[23] A.J. Marchi, C.R. Apesteguía, Applied Clay Science 13 (1998) 35–48.
[24] A.J. Marchi, J.L.G. Fierro, J. Santamaría, A. Monzón, Applied Catalysis A-General 142 (1996) 375–386.
[25] H. Rojas, G. Borda, D. Rosas, J.J. Martínez, P. Reyes, Dyna 155 (2008) 115–122.